Characterization of the Pore Structure and Surface Properties of Shale Using the Zeta Adsorption Isotherm Approach

ARTICLE *in* ENERGY & FUELS · APRIL 2015

Impact Factor: 2.79 · DOI: 10.1021/acs.energyfuels.5b00244

2 AUTHORS:

Hadi Zandavi

University of Toronto

5 PUBLICATIONS **13** CITATIONS

SEE PROFILE

Charles Albert Ward

University of Toronto

141 PUBLICATIONS **2,587** CITATIONS

SEE PROFILE

energy&fuels

Article

pubs.acs.org/EF

Characterization of the Pore Structure and Surface Properties of Shale Using the Zeta Adsorption Isotherm Approach

Seyed Hadi Zandavi and C. A. Ward*

Thermodynamics and Kinetics Laboratory, Department of Mechanical and Industrial Engineering, University of Toronto, 5 King's College Road, Toronto, Ontario M5S 3G8, Canada

ABSTRACT: The determination of the specific surface area and pore structure parameters of natural materials have been a long-standing issue. We propose a method for determining the specific surface area and pore size distribution that is based on the zeta adsorption isotherm and apply that method for each of two hydrocarbon vapors, octane and heptane, adsorbing on two types of shale, as-received and milled shale. We determined the specific surface areas of both materials, approximate the pores as cylindrical, and determine the average pore mouth radius. The standard deviation in the mean values of the specific surface areas and average pore radius determined with each of the two vapors is less than 3%. The experimental isotherms on the as-received shale indicate the existence of a pronounced adsorption−desorption hysteresis loop that results from the mesoporous structure of the material. We previously showed that liquid forms in the pores because of coalescence of molecular clusters inside the pores. In this study, we show that the pore emptying in the as-received shale is delayed because of the pore blocking effect. The zeta isotherm theory and the necessary conditions for thermodynamic equilibrium along with the measured amount adsorbed are used to determine the distribution in the pore mouth radii.

1. INTRODUCTION

Our objective is to use the zeta adsorption isotherm (ZAI) with the Kelvin equation to determine the pore structure of "deep earth core" shale. The theoretical ZAI is based on the concept of the adsorbate consisting of adsorbed molecular clusters.[1−3] It indicates that, at each x^V (≡vapor-phase pressure divided by the saturation vapor, P_s), the adsorbate consists of differently sized molecular clusters. The Kelvin equation predicts that the contact angle depends upon the pressure. We take this effect fully into account and show that it is particularly important in determining the pore mouth radius.[3]

The assumptions made leading to ZAI are in contrast to those leading to the other theoretical isotherms, such as Brunauer−Emmett−Teller (BET) isotherm, that assume that the adsorbate is in layers.[4−6] A remarkable difference between approaches is seen in the amount predicted to be adsorbed in the limit of x^V approaching unity and for x^V greater than unity. Those isotherms that assume the adsorbate is in layers indicate that an infinite amount is adsorbed in this limit of x^V approaching unity[5] and that the amount adsorbed is predicted to be negative when x^V is greater than unity. In contrast, the ZAI indicates that the amount adsorbed when x^V is equal to unity is finite and that, when x^V is greater than unity, an adsorbed vapor film forms.[7]

We have previously investigated the validity of the ZAI to determine the material properties of standard materials. These properties include the specific surface area of a nonporous silica (Aerosil 150) and two mesoporous silicas (MCM-41[8] and SBA-15[9]) and the average pore diameter of these mesoporous silicas.[3,10] We have tested this approach further using it to propose the mechanism of capillary condensation in mesoporous materials exposed to different vapors (water and three hydrocarbons).[10]

From the vapor adsorption isotherms of nonporous milled shale samples and the porous as-received sample, we demonstrate that the ZAI can be used to predict the pore structure and distribution of the pore mouth radii. We show that the average pore radius is 1.90 ± 0.03 nm, the average pore volume is 80 ± 4 nm^3, the total volume of the mesopores is 0.017 ± 0.001 mm^3/mg, and the specific surface area of the as-received shale is 22.5 ± 0.5 m^2/g.

2. MATERIALS AND METHODS

The shale samples used in this study were supplied by Schlumberger. The major elements in the composition of the shale were determined by a X-ray fluorescence (XRF) spectrometer. The chemical composition of the shale sample is presented in Table 1. The XRF elemental analysis indicates that Si, Al, Fe, K, Na, and Mg are the major elements present in the shale. The results from the XRF method also show that the shale has a high concentration of oxides: SiO_2, Al_2O_3, Fe_2O_3, K_2O, and MgO.

Table 1. XRF Analyses of the Shale Sample

element	Na	Mg	Al	Si	K	Fe
compound	Na_2O	MgO	Al_2O_3	SiO_2	K_2O	Fe_2O_3
concentration (%)	1.25	1.71	17.15	66.73	3.46	4.34

Phase and structural state analyses of the material(s) found in the shale sample were performed using the X-ray diffraction (XRD) method. The results revealed the presence of quartz, SiO_2 (33%), and the other silicate mineral, illite (66%).

3. ADSORPTION OF HYDROCARBON VAPORS ON SHALE

We measured the gravimetric adsorption−desorption isotherms of octane and heptane vapors on both the as-received and milled shale samples.

Received: January 30, 2015
Revised: April 3, 2015

DOI: 10.1021/acs.energyfuels.5b00244
Energy Fuels XXXX, XXX, XXX−XXX

3.1. Adsorption of Hydrocarbon Vapors on the Milled Shale. A milled and homogenized shale sample was prepared by grinding the as-received shale samples using vibratory disc mills, which reduced the size of the shale particles to a micrometer-sized powder. The dynamic light scattering (DLS) technique (Zetasizer Nano, Malvern) was used to measure the particle size distribution of the milled shale.

In preparation for the particle size distribution measurements, a few milligrams of the milled shale was placed in a glass vial and the vial was filled with ethanol and placed in an ultrasonic bath for 5 min to disperse the shale in the suspension. Then, the diluted solution was transferred to a square cuvette for DLS measurements. The DLS result is shown in Figure 1. The average particle diameter of the milled shale was 935 nm, and the shale powder mainly ranged between 0.5 and 2 μm.

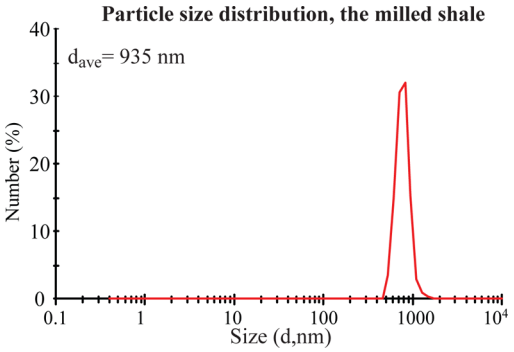

Figure 1. Particle size distribution of the milled shale.

In preparation for measuring the adsorption−desorption isotherm, the milled shale samples were placed in the microbalance of the adsorption instrument (Surface Measurement Systems, DVS Advantage), heated to 523 K, and held at this temperature for 4 h. Then, each sample was cooled to 298 K and exposed to a hydrocarbon vapor at x^V values from near zero to 0.95 ± 0.01.

At each pressure, the value of x^V was held constant until the sample mass did not change by more than 0.02% in the last 15 min or a period of 180 min had expired. If there were no changes (≤0.02%) in weight during the last 15 min of this period, the data point was assumed to be an equilibrium measurement. If there were still changes in the sample weight after this time, the data were considered as a non-equilibrium measurement.

The amount of octane vapor adsorbed per unit weight of the milled shale, n^g_{SV}, is shown in Figure 2A. Equilibrium was achieved at each x^V. The adsorption−desorption isotherm of octane on the milled shale sample was almost reversible. This isotherm is classified as type II of the International Union of Pure and Applied Chemistry (IUPAC)[11] classification, and it indicates that the milled shale is nonporous.

The adsorption measurements shown in Figure 2A were employed to determine the ZAI constants. The ZAI[1,12] expression has x^V as its independent variable and contains four temperature-dependent constants: M_g, ζ_m, c, and α.

$$n_g^{SV} = \frac{M_g c\alpha x^V[1 - (1+\zeta_m)(\alpha x^V)^{\zeta_m} + \zeta_m(\alpha x^V)^{1+\zeta_m}]}{(1-\alpha x^V)[1 + (c-1)\alpha x^V - c(\alpha x^V)^{1+\zeta_m}]} = M_g f(x^V, c, \alpha, \zeta_m) \quad (1)$$

In this equation, n_g^{SV} is the amount adsorbed per unit mass of the adsorbent, M_g is the number of adsorption sites per unit weight of a solid substrate, ζ_m is the maximum number of molecules in any adsorbed cluster, and c and α are two dimensionless, temperature-dependent parameters.

The discrepancy between the ZAI predictions, n_g^{SV}, and the measured values, n_m^{SV}, may be assessed using an error estimate, $\Delta(\zeta_m)$[1,3,12]

$$\Delta(\zeta_m) \equiv \frac{\sqrt{\sum_{j=1}^{N_m}[n_m^{SV}(x_j^V) - n_g^{SV}(x_j^V, M_g, c, \alpha, \zeta_m)]^2}}{\sum_{j=1}^{N_m} n_m^{SV}(x_j^V)} \quad (2)$$

where N_m is the number of equilibrium measurements in each adsorption or desorption cycle. We follow the procedure outlined in ref 1 and use the nonlinear regression package of Mathematica to determine the values of M_g, c, α, and ζ_m that minimizes the difference between the measured isotherm and that calculated from eq 1. The value of $\Delta(\zeta_m)$ for octane adsorbing on the milled shale was calculated to be 0.4% (Table 2). Figure 2A shows that the recalculated ZAI agrees closely with the input data.

The adsorption−desorption isotherm of heptane vapor on this substrate is similar (Figure 2B). Also listed in Table 2 are the zeta isotherm parameters for heptane adsorbing on the milled shale. The adsorption−desorption isotherm of octane and heptane vapors on the milled shale was measured a second time, but no

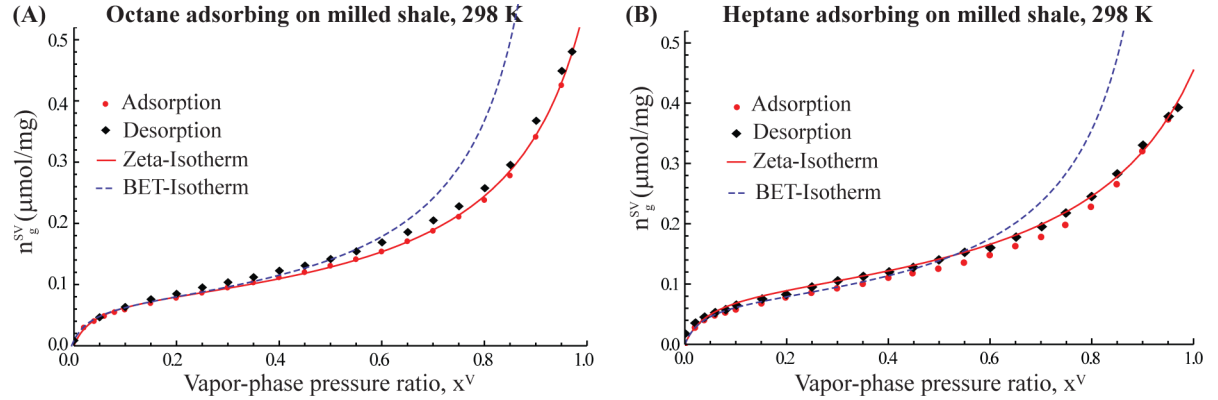

Figure 2. Adsorption−desorption isotherms of (A) octane and (B) heptane on the milled shale. The recalculated zeta isotherms are shown as the red lines. The dashed lines were calculated from the BET isotherm. Equilibrium was achieved at each x^V.

DOI: 10.1021/acs.energyfuels.5b00244
Energy Fuels XXXX, XXX, XXX−XXX

Table 2. Zeta Isotherm Constants for Octane or Heptane Vapor on the Milled Shale at 298 K

vapor	M_g (μmol/mg)	A_s(mshale) (m^2/g)	M (μmol/m^2)	c	α	ζ_m	error $\Delta(\zeta_m)$ (%)
octane	0.076 ± 0.002	35 ± 2	2.17 ± 0.05	31 ± 5	0.868 ± 0.008	65	0.38
heptane	0.089 ± 0.003	34 ± 2	2.62 ± 0.05	27 ± 4	0.806 ± 0.005	80	0.65
mean		34.5 ± 0.5					

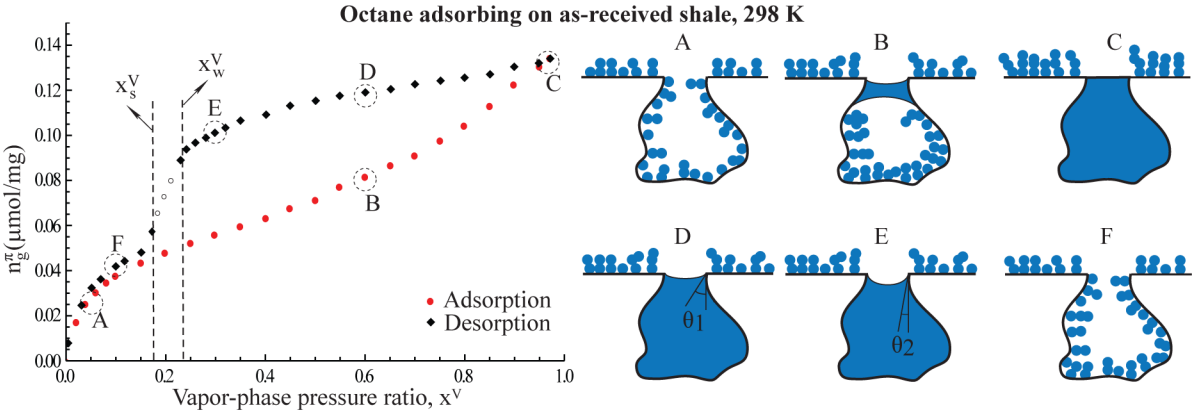

Figure 3. Octane adsorbing on the as-received shale. An open circle indicates that equilibrium was not reached in 3 h of observation. x_w^V is the pressure at which the contact angle of the liquid phase is zero, and x_s^V is the pressure of the highest equilibrium measurement at which no confined liquid phase is present in a pore. Schematic diagrams of the adsorption and desorption processes in a pore of the shale are shown.

measurable discrepancy was found with the first measurements. Thus, the zeta isotherm is also repeatable and reversible.

3.2. Adsorption of Hydrocarbon Vapors on the As-Received Shale. We performed hydrocarbon vapor adsorption−desorption experiments on the as-received shale samples. The preheating procedure and criterion for equilibrium in the measurements were the same as that for the milled shale. The measured amounts of octane adsorbed per unit weight of the as-received shale, n_g^π, are shown in Figure 3. If equilibrium was achieved during the adsorption process, the data point is shown as a filled symbol, and if equilibrium was not achieved during the adsorption process, the data point is shown by an open symbol.

In Figure 3, there is a wide hysteresis loop between the adsorption and desorption measurements on the as-received materials. This hysteresis loop is clearly different from the hysteresis loops that were found earlier[10] in MCM-41 and SBA-15. This hysteresis loop may be related to the "pore-blocking" effect[15−17] (see Figure 3). When this occurs, the interior pores in the sample are unable to empty during desorption because they are not connected to the exterior vapor volume[18] (see Figure 3). The pore-blocking effect is widely used to describe the hysteresis phenomenon in random porous materials.[14] Because the shale sample was heated before the adsorption experiment, the pore-blocking mechanism did not affect the adsorption branch of the isotherm.[18]

It was found that 0.008 μmol/mg of octane remained adsorbed even after exposing the as-received shale sample to dry nitrogen for a period of 30 h. This phenomena indicates that some octane was trapped.[19] We emphasize that this residual octane may be related to the microporosity[20] of the shale sample, which we neglect.

The adsorption−desorption isotherm of heptane vapor on the as-received shale was similar (Figure 4). The adsorption−desorption isotherm of octane and heptane vapors on the shale sample was measured for a second time. There was no measurable discrepancy with the first measurements.

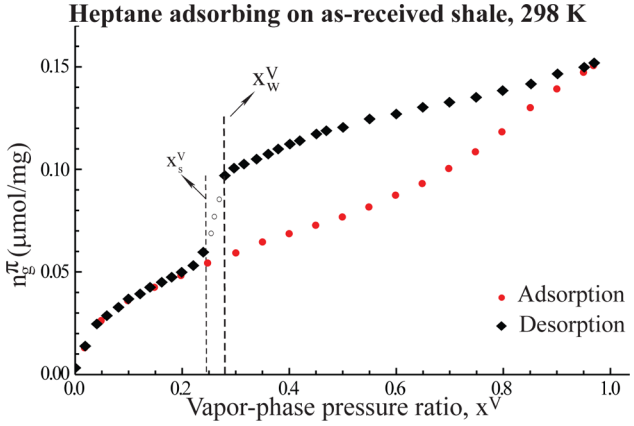

Figure 4. Heptane adsorbing on the as-received shale. An open circle indicates that equilibrium was not reached in 3 h of observation. x_w^V is the pressure at which the contact angle of the liquid phase is zero, and x_s^V is the pressure of the highest equilibrium measurement at which no confined liquid phase is present in a pore.

4. RESULTS

The values of the material properties, such as the specific surface areas, the average pore radius, and the distribution of the pore mouth radii, should be independent of the vapor used to determine them. We test the approach being developed by determining the value of these material properties using each of the two hydrocarbon vapors.

4.1. Surface Area Ratio of the As-Received Shale to the Milled Shale. In comparison of the octane adsorption and desorption isotherms on the milled shale (Figure 2) and the as-received sample (Figure 3), one can conclude that the grinding process almost destroyed the mesopores in the as-received shale.

The intensive zeta isotherm constants listed in Table 2 are material properties of the milled shale.[3] Because the milled shale is prepared from the as-received shale and there is no condensate phase of the vapor in the mesopores of the as-received shale for

DOI: 10.1021/acs.energyfuels.5b00244
Energy Fuels XXXX, XXX, XXX−XXX

$x^V \le x_s^V$ (see Figures 3 and 4), the intensive ZAI constants can be used to predict the amount adsorbed per unit area of the as-received shale in the pressure range considered. The milling process increases the specific surface area of the shale, but it does not change the intensive zeta isotherm constants, M, c, α, and ζ_m, where M is the number of adsorption sites per unit area of the solid substrate.

According to the ZAI and for the amount adsorbed per unit area of the milled shale, n^{SV}, one can write

$$n^{SV} = \frac{n_g^{SV}}{A_s(\text{mshale})} = \frac{M_g}{A_s(\text{mshale})} f(x^V, c, \alpha, \zeta_m) = Mf(x^V, c, \alpha, \zeta_m) \quad (3)$$

where A_s(mshale) is the specific surface area of the milled shale. For the as-received shale in the considered range of vapor-phase pressure, $0 \le x^V \le x_s^V$, we arrive at

$$n^{\pi} = \frac{n_g^{\pi}}{A_s(\text{shale})} = \frac{M_g^{\text{shale}}}{A_s(\text{shale})} f(x^V, c, \alpha, \zeta_m) = M f(x^V, c, \alpha, \zeta_m) \quad (4)$$

where n^{π} is the amount of vapor adsorbed per unit area of the as-received shale and A_s(shale) is the surface area of as-received shale. These two intensive properties, n^{SV} and n^{π}, are equal, and one may write[3]

$$\frac{A_s(\text{shale})}{A_s(\text{mshale})} = \frac{n_g^{\pi}}{n_g^{SV}} \quad (5)$$

Because n_g^{π} has been directly measured and n_g^{SV} can be calculated using the ZAI, the specific surface area ratio may be determined at the same value of x^V. This ratio, A_s(shale)/A_s(mshale), should be a constant. As seen in Table 3, the specific specific area ratio is almost constant. The mean is 0.65 with a standard deviation of 5%.

Table 3. Ratio of A_s(shale)/A_s(mshale) for Octane Adsorption on Shales for $x^V \le x_s^V$ at 298 K

x^V	n_g^{π}/n_g^{SV}	x^V	n_g^{π}/n_g^{SV}
0.02	0.585	0.10	0.627
0.04	0.653	0.12	0.652
0.06	0.665	0.14	0.674
0.08	0.675		
		mean ± SDV	0.65 ± 0.03

4.2. Average Properties of the As-Received Shale. For the as-received shale, we model the pores as uniform cylindrical pores with an average radius of $\overline{r}_p$ and average pore volume of $\overline{v}_p$. We also determine the specific number of pores, η_g, and the specific surface areas, A_s(shale) and A_s(mshale).

When the liquid phase of the hydrocarbon is formed inside a pore, the Laplace equation and the equality of the chemical potentials of each phase across the liquid−vapor interface are the two necessary conditions for equilibrium. If the specific volumes of the liquid and vapor phases are denoted as v_f and v_g, then the average pore radius can be calculated from[10]

$$\overline{r}_p = \frac{2\gamma^{LV}\cos\theta}{P_s\left(x^V - 1 - \frac{v_f}{v_g}\ln x^V\right)} \quad (6)$$

where θ is the contact angle of the liquid phase with the pore wall and γ^{LV} is the liquid−vapor surface tension. Historically, θ has been assumed to be independent of the pressure in the liquid at the three-phase line,[21] but this assumption is not supported by recent experiments.[3,7,22−25]

We have shown in our previous publications[3,10] that, for the mesoporous silicas (MCM-41 and SBA-15), with average pore diameters of 2.6 and 6.7 nm, the contact angle of the confined liquid phase is zero when the vapor-phase pressure is at x_w^V, pore-emptying pressure. We assume that the hydrocarbon liquid forms a contact angle of zero with a shale pore wall at x_w^V as well (Table 4). The average pore radius of the as-received shale calculated from eq 6 is listed in Table 4. As seen there, the mean pore mouth radius is 1.90 nm and the standard deviation in values (SDV) obtained is less than 3.0%.

In our model, when the vapor-phase pressure is at its maximum value (a value near unity), the contact angle is 90° and all of the assumed uniformly sized pores are totally filled by the liquid phase of the hydrocarbon (Figure 3). During the desorption and when the pressure in the vapor phase is at an intermediate pressure between unity and x_w^V, the liquid phase forms a contact angle of θ with the pore wall (Figure 3). The experimentally measured values of n_g^{π} in this pressure range are a summation of the weight of the condensed liquid phase in the pores and the amount adsorbed on the area exterior to the pores, A_s(xt). The amount adsorbed on this surface area can be calculated from the ZAI of the milled shale sample. The volume of the confined liquid in a pore at each value of x^V, $v^L[\overline{r}_p, \theta(x^V)]$, can be found from the geometry.

We follow the procedure outlined in our previous paper[3] and form a set of three coupled equations that may be solved simultaneously to obtain the specific number of pores, η_g, an average volume of the pore, $\overline{v}_p$, and the external surface area to the pores, A_s(xt). Once these values are known, the average pore depth, $\overline{z}_p = \overline{v}_p/\pi\overline{r}_p^2$, the total mesoporous volume, V_p, and the value of A_s(shale) may be obtained, and then finally from eq 5, the value of A_s(mshale) may be determined.

For octane and heptane adsorbing on the shale samples, the values of these parameters are listed in Tables 2 and 4. The error bars listed in Table 4 result from the limit on the accuracy of the pressure measurements ($\Delta x^V = \pm 0.01$).

The consistency of these values can be examined by comparing the results to results determined using different vapors in the adsorption experiments. We assess the procedure by considering the consistency of the property values obtained with two vapors, octane and heptane (Tables 3 and 4) and find that the properties differ by only a few percentages.

Table 4. Pore Radius, Volume, and the Specific Surface Area of the As-Received Shale Sample

vapor	x_w^V	$\overline{r}_p$ (nm)	$\overline{z}_p$ (nm)	$\overline{v}_p$ (nm^3)	η_g (×10^{14}, mg^{-1})	A_s(xt) (m^2/g)	A_s(shale) (m^2/g)	V_p(shale) (mm^3/mg)
octane	0.24 ± 0.01	1.93 ± 0.04	7.2 ± 0.4	84 ± 4	2.1 ± 0.2	2.9 ± 0.3	23 ± 2	0.018 ± 0.001
heptane	0.28 ± 0.01	1.87 ± 0.04	6.9 ± 0.4	76 ± 3	2.0 ± 0.2	3.3 ± 0.3	22 ± 2	0.016 ± 0.001
mean		1.90 ± 0.03	7.1 ± 0.2	80 ± 4	2.0 ± 0.1	3.1 ± 0.2	22.5 ± 0.5	0.017 ± 0.001

DOI: 10.1021/acs.energyfuels.5b00244
Energy Fuels XXXX, XXX, XXX−XXX

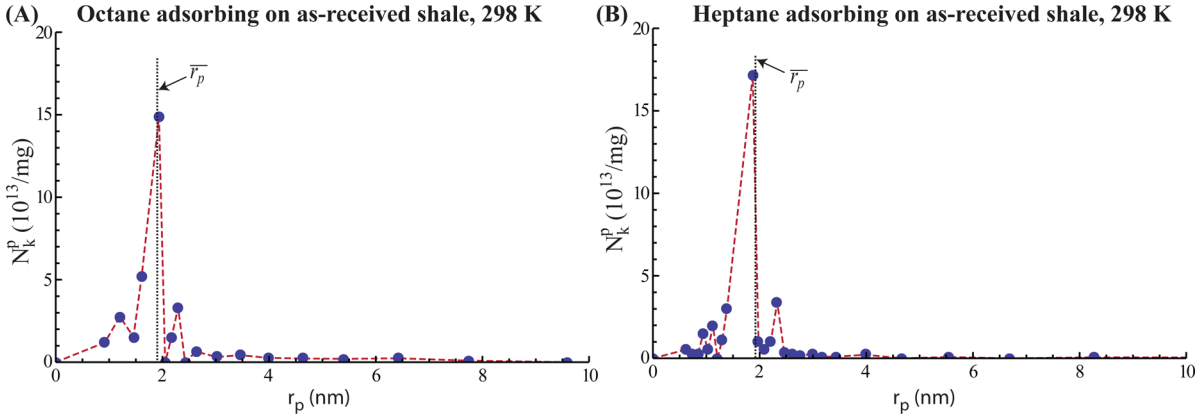

Figure 5. Pore mouth radii distribution in the as-received shale determined by (A) octane and (B) heptane vapor adsorptions.

4.3. Determination of the Distribution in the Pore Mouth Radii. The method described in the previous section gives the average pore radius of the as-received shale, $\overline{r}_p$, with an error of 4% (Table 4). In this section, we extend the method to determine the spread in the pore mouth radii in the as-received shale.

If x_j^V denotes the vapor-phase pressure when measurement j was made and there are a total of N_m equilibrium desorption measurements, then $1 \le j \le N_m$. Pores with different mouth radii may exist in a porous structure, and pore emptying may occur in them at different pressures.

In this model, the total amount adsorbed and confined at x_j^V is denoted as $n_g^\pi(x_j^V)$. As seen in eq 7, $n_g^\pi(x_j^V)$ is a summation of three terms: term i is the amount of liquid phase in the pores with mouth radii less than r_j; term ii is the amount adsorbed on the walls of the bigger sized pores in which no confined liquid phase is present; and term iii is the amount adsorbed in the areas exterior to the pores.

$$n_g^\pi(x_j^V) = \underbrace{\sum_{k=1}^{j} \frac{N_k^p v_k^L(x_j^V, r_k)}{v_f}}_{\text{i}} + \underbrace{\sum_{k=j+1}^{N_m} N_k^p A_k^p n^{SV}(x_j^V, M, c, \alpha, \zeta_m)}_{\text{ii}} + \underbrace{A_s(xt) n^{SV}(x_j^V, M, c, \alpha, \zeta_m)}_{\text{iii}} \quad (7)$$

In eq 7, N_k^p is the specific number of pores with the mouth radius of r_k, $v_k^L(x_j^V, r_k)$ is the volume of the liquid phase in a pore with radius r_k when the pressure is x_j^V, and A_k^p is the surface area of a pore with the radius of r_k.

The pore mouth radius, r_k, can be calculated from the Kelvin equation (eq 6) by assigning $\theta = 0$ at x_k^V. The volume of the confined liquid in a pore, v_k^L, may be calculated from the geometry as

$$v_k^L(x_j^V, r_k) = \pi r_k^2 \overline{z}_p - V_c(r_k, x_j^V) \quad (8)$$

where V_c is the volume of the spherical vapor cap.[3]

$$V_c(r_k, x_j^V) = \frac{1}{3}\pi \left(\frac{r_k}{\cos[\theta(r_k, x_j^V)]} \right)^3 (1 - \sin[\theta(r_k, x_j^V)])^2 (2 + \sin[\theta(r_k, x_j^V)]) \quad (9)$$

Also, the surface area of a pore with a mouth radius of r_k is simply

$$A_k^p = 2\pi r_k \overline{z}_p + \pi r_k^2 \quad (10)$$

Once the ZAI constants are measured for a vapor on the milled shale, one may obtain an explicit expression for $n^{SV}(x_j^V, M, c, \alpha, \zeta_m)$. Then, the desorption branch of the isotherm on the as-received shale may be used to determine the pore size distribution in the shale. This requires that eq 7 is to be written for each of the N_m desorption measurements. Thus, one obtains N_m equations. These equations may be solved simultaneously to determine the values of N_k^p, where $k = 1, 2, ..., N_m$. We emphasize that equilibrium should be reached at each of the N_m desorption measurements.

The distribution of the pore mouth radii in the as-received shale determined from octane desorption measurements is shown in Figure 5A. The mesopores in the as-received shale are almost uniform in size. There is no measurable difference between the pore mouth radius measured by assuming uniform pores and the results from the pore size distribution.

The consistency of the pore size distribution obtained from octane adsorption measurements was examined by comparing the results to results determined using heptane vapor in the adsorption experiment. As seen from Figure 5, the predicted pore radii distribution obtained from the measurements with each vapor gave very consistent results.

4.4. BET Specific Surface Area. In the BET isotherm formulation, the conception was that adsorption takes place in layers. As x^V is increased from zero, the adsorbate was assumed to first form a monolayer, and then with a further increase in x^V, the molecules were suggested to adsorb on the monolayer to form a second layer and possibly higher layers. The BET isotherm gives a valid description of the adsorption on a nonporous material only in a limited x^V range. Figure 2 shows a comparison between the BET and the ZAI. As expected, the BET isotherm only describes the measurement data for $x^V \le 0.55$, but the ZAI is found to accurately describe the adsorption for $0 < x^V < 1$.

The BET isotherm is usually applied at 77 K with N_2 adsorbing. The BET surface area is determined from the assumption that, under certain conditions, a monolayer is formed. With knowledge of the cross-section of the N_2 molecule

DOI: 10.1021/acs.energyfuels.5b00244
Energy Fuels XXXX, XXX, XXX−XXX

Table 5. Porosity of the As-Received Shale Sample Measured at 295 K

V_s (cm^3)	W_d (g)	W_{wet} (g)	V (cm^3)	ρ(shale) (g/cm^3)	Φ (%)	ϕ_{meso} (%)
2.26 ± 0.09	6.28 ± 0.02	3.7 ± 0.3	2.52 ± 0.20	2.47 ± 0.09	10.3 ± 0.9	4.2 ± 0.5

and estimation of the number of molecules adsorbed in the monolayer, the surface area can be estimated. It had been thought to have an accuracy of 20%,[11] but recent work has raised doubts about the method because it does not give consistent results when different vapors are used in the determination.[13]

We used the instrument software of Surface Measurement Systems (London, U.K.) to obtain the BET surface areas of the milled shale from the adsorption measurements of the two vapors, heptane and octane, in the pressure range of $0 \leq x^V \leq 0.35$ at 298 K. This software indicated that the BET surface area was 32 m^2/g for heptane and 28 m^2/g for octane adsorption measurements or a difference of 13% between the two values.

The values of the specific surface areas that we calculated from the ZAI are listed in Table 2. There is no statistical difference between the two surface areas obtained from heptane and octane adsorption measurements. The ZAI surface area could be reported as 34.5 ± 0.5 m^2/g or 34.5 ± 2% m^2/g.

4.5. Porosity Measurements. The total shale porosity is defined as the ratio of the volume of all pores in the shale, V_{pt}, to the bulk volume of the shale, V. The shale porosity, Φ, was measured using the following equation:[26]

$$\Phi = \frac{V - V_s}{V} \times 100 = \frac{V_{pt}}{V} \times 100 \tag{11}$$

where V_s is the net solid volume of the shale.

We used the gas-expansion technique (Quantachrome, Ultrapycnometer 1000) to measure the net solid volume of an as-received shale sample, V_s (Table 5). The bulk volume, V, of the shale was measured using a density determination kit (Denver Instruments). If the weight of the as-received shale sample in air (dry weight) is denoted as W_d and its weight immediately after it is fully immersed in water is denoted as W_{wet}, then the bulk volume can be calculated from

$$V = \frac{W_d - W_{wet}}{\rho_{water}} \tag{12}$$

where ρ_{water} is the density of water at the experimental conditions. The total porosity of the as-received shale sample was measured to be approximately 10% (Table 5) using the above-mentioned procedure.

Also listed in Table 5 is the shale bulk density, which is defined as

$$\rho(\text{shale}) = \frac{W_d}{V} \tag{13}$$

The error bars in Table 5 represent the standard deviations of five independent experiments.

The mesoporosity of the as-received shale can be defined as

$$\phi_{meso} = V_p(\text{shale})\rho(\text{shale}) \times 100 \tag{14}$$

and its value is also listed in Table 5. The difference between the values of the total porosity (Φ) and the mesoporosity (ϕ_{meso}) in the shale indicates the presence of "macroporosity"[27] ($2r_p \geq 50$ nm). In the pores with these radii, pore filling or emptying occurs at pressures very close to the saturation vapor-phase pressure. Pores in this range cannot be detected by the vapor adsorption techniques. Only the surface area of the macropores was measured in our procedure.

5. CONCLUSION

The adsorption−desorption isotherms for each of two vapors (heptane and octane) on both the as-received and milled shale have been measured. For the as-received shale, the adsorption−desorption isotherms exhibited a large hysteresis loop. This is an indication of the existence of the mesoporous structure in the as-received shale.

The adsorption−desorption isotherms for the two vapors on the milled shale were almost reversible. Thus, one can conclude that the milling process destroyed the mesoporus structure in the shale. The zeta adsorption isotherm was applied and shown to give an excellent description of the amount of vapor adsorbed on and desorbed from the milled shale.

The ZAI was added to Gibbsian thermodynamics to form a theoretical model that can be used to determine the material properties of "deep earth core" shale. The necessary conditions for thermodynamic equilibrium were used to determine θ as a function of x^V and $\overline{r}_p$.

For the two vapors considered in this study, the average value of the pore mouth radius, $\overline{r}_p$, of the as-received shale was accurately determined from the desorption isotherm of each vapor by assuming that, at the minimum pressure of the cycle reached with condensate at the pore mouth, x_w^V, the contact angle was zero. When the Kelvin equation was applied at this condition, the pore radius was found to be 1.90 nm and the standard error in this value was only 2%.

Further, the experimentally measured desorption isotherms on the as-received shale were applied to the theoretical model to determine the other material properties of the shale. We found that shale has a specific surface area of 22.5 m^2/g with an error of only 3%. The pore mouth size distributions obtained from octane and heptane adsorption measurements agree closely with each other. The consistency between the values of material properties obtained from the two hydrocarbons supports the dependence of the contact angle upon the pressure and also supports the hypothesis that Gibbsian thermodynamics can be applied in nano-sized pores with mouth radii as small as 1.90 nm.

AUTHOR INFORMATION

Corresponding Author

*E-mail: charles.ward@utoronto.ca.

Notes

The authors declare no competing financial interest.

ACKNOWLEDGMENTS

The authors are grateful to Dr. Mark Andersen from Schlumberger, Ltd. for helpful conversations regarding this work and gratefully acknowledge the support received from Schlumberger Canada, Ltd. and the Natural Sciences and Engineering Research Council of Canada.

NOMENCLATURE

P^V = vapor-phase pressure
P_s = saturation vapor pressure

DOI: 10.1021/acs.energyfuels.5b00244
Energy Fuels XXXX, XXX, XXX−XXX

A_s = specific surface area
$A_s(xt)$ = specific surface area exterior to the pores
γ^{LV} = liquid−vapor surface tension
v_g = specific volume of the vapor at saturation
$\overline{z}_p$ = average pore depth
N_k^p = number of pores with the radius of r_k
M = zeta adsorption isotherm constant
V_c = volume of the spherical vapor cap
V = bulk volume of the shale
V_s = solid volume of the shale
W_{wet} = wet weight
n^{SV} = vapor adsorption per unit area (nonporous)
n_g^{SV} = vapor adsorption per weight (nonporous)
$\overline{r}_p$ = average pore radius
x^V = vapor-phase pressure ratio
x_w^V = vapor-phase pressure when $\theta = 0$
V_p = total mesoporous volume
v_f = specific volume of the liquid at saturation
$\overline{v}_p$ = average pore volume
N_m = number of equilibrium measurements
A_k^p = surface area of a pore with the radius of r_k
c = zeta adsorption isotherm constant
x_s^V = pore-filling pressure
V_{pt} = total pore volume
W_d = dry weight
v_k^L = volume of the liquid phase in a pore
n^π = vapor adsorption per surface area (porous)
n_g^π = vapor adsorption per weight (porous)

Greek Letters

α = zeta adsorption isotherm constant
ζ_m = maximum number of molecules in a cluster
Φ = total shale porosity
Δ = error function
θ = contact angle
ρ = density
ϕ_{meso} = porosity in the meso range
η_g = specific number of pores

REFERENCES

(1) Ward, C. A.; Wu, J. *J. Phys. Chem. B* **2007**, *111*, 3685−3694.
(2) Ward, C. A.; Wu, J. *Phys. Rev. Lett.* **2008**, *100*, 256103.
(3) Zandavi, H.; Ward, C. A. *J. Colloid Interface Sci.* **2013**, *407*, 255−264.
(4) Brunauer, S.; Emmett, P. H.; Teller, E. *J. Am. Chem. Soc.* **1938**, *60*, 309−319.
(5) Masel, R. I. *Principles of Adsorption and Reaction on Solid Surfaces*; John Wiley & Sons, Inc.: New York, 1996.
(6) Adamson, A. W. *Physical Chemistry of Surfaces*, 2nd ed.; John Wiley & Sons, Inc.: New York, 1960.
(7) Wu, C.; Zandavi, S. H.; Ward, C. A. *Phys. Chem. Chem. Phys.* **2014**, *16*, 25564−25572.
(8) Kresge, C. T.; Leonowicz, M. E.; Roth, W. J.; Vartuli, J. C.; Beck, J. S. *Nature* **1992**, *359*, 710−712.
(9) Zhao, D.; Feng, J.; Huo, Q.; Melosh, N.; Fredrickson, G. H.; Chmelka, B. F.; Stucky, G. D. *Science* **1998**, *279*, 548−542.
(10) Zandavi, S. H.; Ward, C. A. *Phys. Chem. Chem. Phys.* **2015**, *17*, 9828−9834.
(11) Sing, K. S. W.; Everett, D. H.; Haul, R. A. W.; Moscou, L.; Pierotti, R. A.; Rouquérol, J.; Siemieniewska, T. *Pure Appl. Chem.* **1985**, *57*, 603−619.
(12) Zandavi, S. H.; Ward, C. A. *Phys. Chem. Chem. Phys.* **2014**, *16*, 10979−10989.
(13) Matejova, L.; Solcova, O.; Schneider, P. *Microporous Mesoporous Mater.* **2008**, *107*, 227−232.
(14) Valiullin, R.; Karger, J.; Glaser, R. *Phys. Chem. Chem. Phys.* **2009**, *11*, 2833−2853.
(15) Nguyen, P. T. M.; Fan, C.; Do, D. D.; Nicholson, D. *J. Phys. Chem. C* **2013**, *117*, 5475−5484.
(16) Ravikovitch, P. I.; Neimark, A. V. *Langmuir* **2002**, *18*, 1550−1560.
(17) Coasne, B.; Galarneau, A.; Pellenq, R. J. M.; Di Renzo, F. *Chem. Soc. Rev.* **2013**, *42*, 4141−4171.
(18) Qi, H.; Ma, J.; zen Wong, P. *Colloids Surf.* **2002**, *206*, 401−407.
(19) Khraisheh, M.; Al-Ghoutib, M.; Allenb, S.; Ahmadb, M. *Water Res.* **2005**, *39*, 922−932.
(20) Mastalerz, M.; He, L.; Melnichenko, Y. B.; Rupp, J. A. *Energy Fuels* **2012**, *26*, 5109−5120.
(21) Zisman, W. A. Relation of the equilibrium contact angle to liquid and solid constitution. In *Contact Angle, Wettability and Adhesion*; Fowkes, F. M., Ed.; American Chemical Society (ACS): Washington, D.C., 1964; Advances in Chemistry, Vol. *43*, Chapter 1, pp 1−51.
(22) Good, R. J.; Koo, M. N. *J. Colloid Interface Sci.* **1979**, *71*, 283−292.
(23) Ghasemi, H.; Ward, C. A. *J. Phys. Chem. C* **2010**, *114*, 5088−5100.
(24) Wu, J.; Farouk, T.; Ward, C. A. *J. Phys. Chem. B* **2007**, *111*, 6189−6197.
(25) Ward, C. A.; Wu, J.; Keshavarz, A. *J. Phys. Chem. B* **2008**, *112*, 71−80.
(26) Mosanenzadeh, S. G.; Naguib, H. E.; Park, C. B.; Atalla, N. *J. Appl. Polym. Sci.* **2013**, 39518−39529.
(27) Rouquerol, J.; Avnir, D.; Fairbridge, C. W.; Everett, D. H.; Haynes, J. M.; Pernicone, N.; Ramsay, J. D. F.; Sing, K. S. W.; Unger, K. K. *Pure Appl. Chem.* **1994**, *66*, 1739−1758.

DOI: 10.1021/acs.energyfuels.5b00244
Energy Fuels XXXX, XXX, XXX−XXX